Applied Surface Science 387 (2016) 581–587

Contents lists available at ScienceDirect

Applied Surface Science

journal homepage: www.elsevier.com/locate/apsusc

Effects of porous films on the light reflectivity of pigmentary titanium dioxide particles

Yong Liang, Bing Qiao, Tig-Jie Wang*, Han Gao, Keyi Yu

Department of Chemical Engineering, Tsinghua University, Beijing 100084, China

ARTICLE INFO

Article history:
Received 13 April 2016
Received in revised form 16 June 2016
Accepted 23 June 2016
Available online 25 June 2016

Keywords:
Titanium dioxide
Coating
Porous film
Template
Light reflectivity
Hiding power

ABSTRACT

The light reflectivity of the film-coated titanium dioxide particles (TiO_2) as a function of the film refractive index was derived and calculated using a plane film model. For the refractive index in the range of 1.00–2.15, the lower the film refractive index is, the higher is the light reflectivity of the film. It is inferred that the lower apparent refractive index of the porous film resulted in the higher reflectivity of light, i.e., the higher hiding power of the titanium dioxide particles. A dense film coating on TiO_2 particles with different types of oxides, i.e., SiO_2, Al_2O_3, MgO, ZnO, ZrO_2, TiO_2, corresponding to different refractive indices of the film from 1.46 to 2.50, was achieved, and the effects of refractive index on the hiding power from the model prediction were confirmed. Porous film coating of TiO_2 particles was achieved by adding the organic template agent triethanolamine (TEA). The hiding power of the coated TiO_2 particles was increased from 88.3 to 90.8 by adding the TEA template to the film coating (5–20 wt%). In other words, the amount of titanium dioxide needed was reduced by approximately 10% without a change in the hiding power. It is concluded that the film structure coated on TiO_2 particle surface affects the light reflectivity significantly, namely, the porous film exhibits excellent performance for pigmentary titanium dioxide particles with high hiding power.

1. Introduction

Titanium dioxide (TiO_2) is an excellent white pigment that is widely used in paints, plastics, paper, rubber, ink and other industries. It has three crystal structures in nature, i.e., rutile, anatase and brookite. Rutile titanium dioxide has high hiding power because of its high refractive index. The hiding power represents the ability of TiO_2 particles in a paint layer to cover the background light from the matrix, which is contributed from a large number of TiO_2 particles. It is assumed that high reflectivity of a single TiO_2 particle indicates high reflectivity of the TiO_2 particles in the paint layer. The reflectivity of particles determines the hiding power of particles in the paint layer: high reflectivity corresponds to high hiding power.

However, titanium dioxide also has strong photocatalytic activity: it produces electrons and holes under UV light irradiation, which react with water and oxygen to generate radicals that catalyze and degrade the organic matter around the titanium dioxide particles [1–4]. This results in chalking and life shortening of the painting layer. To increase the weather durability of the TiO_2 particle, the surface needs to be coated with a shield film of inert oxides, e.g., silica and alumina. The co-precipitation method is usually used for the inorganic film coating. By titrating inorganic salts and acid/alkali solution into the TiO_2 suspension, an oxide or hydroxide film is coated on the TiO_2 particle surfaces, which increases the weather durability of TiO_2 particles [5–9].

In our previous work, it was confirmed that the apparent degradation rate coefficient of titanium dioxide with rhodamine-B was reduced as the amount of coating on the TiO_2 particle surface increased. In other words, the weather durability of coated TiO_2 particles increased [10,11]. However, the hiding power of the coated TiO_2 particles decreased as the coating amount increased. The factors affecting the hiding power of titanium dioxide particles were studied and reported in the literature. By using light scattering theory and numerical calculation, Fitzwater et al. [12] and Auger et al. [13] studied the effects of volume fraction of titanium dioxide and the painting thickness on the scattering efficiency of the painted layer to optimize the painting formulation. Veronovski et al. [14] found that TiO_2 particles have a better spatial distribution and scattering efficiency because the porous film-coated TiO_2 parti-

* Corresponding author.
E-mail address: wangtj@tsinghua.edu.cn (T.-J. Wang).

http://dx.doi.org/10.1016/j.apsusc.2016.06.131
0169-4332/

cles have a thicker film structure compared with that of the dense silica-coated TiO_2 particles. This causes the TiO_2 particles coated with porous silicon oxide to have a lower transmittance and higher hiding power.

For TiO_2 particles, the light reflectivity is mainly affected by the difference in refractive indices between core TiO_2 particles and their surroundings. The higher the difference between the refractive indices is, the higher is the light reflectivity of the particles [15]. Theoretically, uncoated TiO_2 particles have high hiding power due to the high difference of refractive indices with their surroundings. However, for film-coated TiO_2 particles, the surrounding of the core TiO_2 particles is the inorganic oxide film (n_1) instead of an organic matrix (n_0), as shown in Fig. 1(a). Generally, the refractive index of the inorganic oxide film (n_1) is higher than that of the organic matrix (n_0), hence, the hiding power of the coated TiO_2 particles decreased because the difference in refractive indices decreased. For the same apparent hiding power, the higher the hiding power of the coated TiO_2 particles was, the lower was the amount of titanium dioxide needed, i.e., the lower the cost. Achievement of high weather durability and high hiding power by fabricating the coated film structure on the TiO_2 particle surface is desired.

The porous films are likely to increase the hiding power of coated TiO_2 particles because of their lower apparent refractive indices compared with the dense films. The preparations of porous alumina have been reported in the literature. Alphonse et al. [16] controlled the specific surface area, pore volume and pore size distribution of porous alumina by adding different organic templates and inorganic ions. Zhu et al. [17] added PEO template in the alumina synthesis process to produce a porous structure. Masoumeh et al. [18] prepared porous alumina with different pore size distributions using different aluminum sources and precipitating agents. Goparaju et al. [19] adjusted the film structure coated on the titanium dioxide particles by controlling the pH in the coating process. Porous alumina structures can be produced by adding different templates and adjusting the preparation process.

In this paper, the change in light reflectivity of the coated film with the film refractive index was calculated using a plane film model. Studies of TiO_2 particles coated with films of various oxides were conducted to verify the prediction of the effects of the refractive index from the model. The porous Si + Al composite film was prepared by addition of the organic template triethanolamine (TEA) and subsequent calcination. The relationship of the pore volume in the coated films on TiO_2 particles surface with the light reflectivity, i.e., hiding power of coated TiO_2 particles, was determined. A low-cost coated titanium dioxide product with high weather durability and high hiding power was prepared.

2. Reflectivity of film-coated TiO_2 particles

When incident light irradiates the surface of a single TiO_2 particle, light reflection, scattering, and absorption occur. For simplification of the analysis, only the reflection and transmittance was considered in the following discussion. Because the thickness of the coated film on the surface of TiO_2 particles is usually less than 20 nm, which is much lower than the TiO_2 particle diameter (approximately 300 nm in average), the spherical film model of a single coated TiO_2 particle was simplified to a plane film model. The reflectivities of coated films with various refractive indices were calculated, and the relationship between the film reflectivity and the film refractive index was determined through a plane film model. As shown in Fig. 1(b), the incident light from the surrounding environment irradiates the coated film surface at an angle of θ_0. The incident light vector is E_0, and the reflected light vectors are E_1, E_2, E_3 ⋯. The optical path difference of any two adjacent reflected lights from the surface of the coated film is $\Delta L = 2n_1 d_1 cos\theta_1$ [20], wherein n_1 is the refractive index of the coated film, d_1 is the coated film thickness, and θ_1 is the angle of refraction. To simplify the analysis, only vertically incident light is discussed below. Then, $\theta_0 = \theta_1 = 0^\circ$ and λ is the wavelength of the incident light, the phase difference is,

$$\delta = 2\pi/\lambda \times 2n_1 d_1 \tag{1}$$

Referring to Fig. 1(b), the reflection coefficients of light on the upper and lower surface of the coated film interfaces 1 and 2 are r_1^+, r_1^-, r_2^+, and r_2^-, respectively. The transmission coefficients are t_1^+, t_1^-, t_2^+, and t_2^-, respectively. Each of the reflected light vectors from the upper surface of interface 1 is,

$$\begin{aligned} E_1 &= r_1{}^+ E_0 \\ E_2 &= t_1{}^+ r_2{}^+ t_1{}^- e^{-j\delta} E_0 \\ E_3 &= t_1{}^+ r_2{}^+ t_1{}^- r_1{}^- r_2{}^+ e^{-j2\delta} E_0 \\ E_4 &= t_1{}^+ r_2{}^+ t_1{}^- \left(r_1{}^- r_2{}^+\right)^2 e^{-j3\delta} E_0 \ldots \end{aligned} \tag{2}$$

According to Eq. (2), the sum of the reflected light vector from the upper surface of interface 1 is,

$$\begin{aligned} lE_R &= \sum_{i=1}^{\infty} E_i \\ &= r_1{}^+ E_0 + t_1{}^+ r_2{}^+ t_1{}^- e^{-j\delta} \left\{1 + r_1{}^- r_2{}^+ e^{-j\delta} + \left(r_1{}^- r_2{}^+ e^{-j\delta}\right)^2 + \ldots\right\} E_0 \\ &= \frac{r_1{}^+ + r_2{}^+ (t_1{}^+ t_1{}^- - r_1{}^+ r_1{}^-) e^{-j\delta}}{1 - r_2{}^+ r_1{}^- e^{-j\delta}} E_0 \end{aligned} \tag{3}$$

According to the Fresnel formula [21], at interface 1,

$$t_1{}^+ \cdot t_1{}^- = 1 - r_1{}^{+2} = 4n_0 n_1/(n_0 + n_1)^2 \tag{4}$$

$$r_1{}^+ = \frac{n_0 - n_1}{n_0 + n_1}, \; r_1^- = -r_1^+ \tag{5}$$

At interface 2,

$$r_2{}^+ = \frac{n_1 - n_2}{n_1 + n_2}, \; r_2^- = -r_2^+ \tag{6}$$

By combining Eqs. (3) and (4), the total reflection coefficient on the coating film of the upper surface is,

$$r = \frac{E_R}{E_0} = \frac{r_1{}^+ + r_2{}^+ e^{-j\delta}}{1 + r_1{}^+ r_2{}^+ e^{-j\delta}} \tag{7}$$

The total reflectivity from the coated film of the upper surface is,

$$R = |r|^2 = \frac{r_1^{+2} + r_2{}^{+2} + 2r_1^+ r_2{}^+ cos\delta}{1 + r_1^{+2} r_2{}^{+2} + 2\, r_1{}^+ r_2{}^+ cos\delta} \tag{8}$$

By combining Eqs. (1), (5), (6) and (8), the film reflectivity was calculated for various thicknesses and refractive indices of the coated film. The curves of coated film reflectivity versus film thickness were obtained, as shown in Fig. 2, by setting the refractive index of the organic matrix n_0 to 1.4; the refractive index of pure rutile titanium dioxide n_2 to 2.75; the film refractive index n_1 to 1.46 (corresponding to silica) or 1.76 (corresponding to alumina); and the wavelengths of incident light λ to 200, 500, and 800 nm. The curves of film reflectivity versus the film refractive index were obtained, as shown in Fig. 3, for a wavelength of the incident light λ at 500 nm; coated film thicknesses d_1 at 5, 10, 20, and 30 nm; and the film refractive index ranging from 1.0 to 2.8.

Fig. 2 shows that the reflectivities of the films corresponding to silica ($n_1 = 1.46$) and alumina ($n_1 = 1.76$) decrease with increasing film thickness under the irradiation of UV light (200 nm), visible

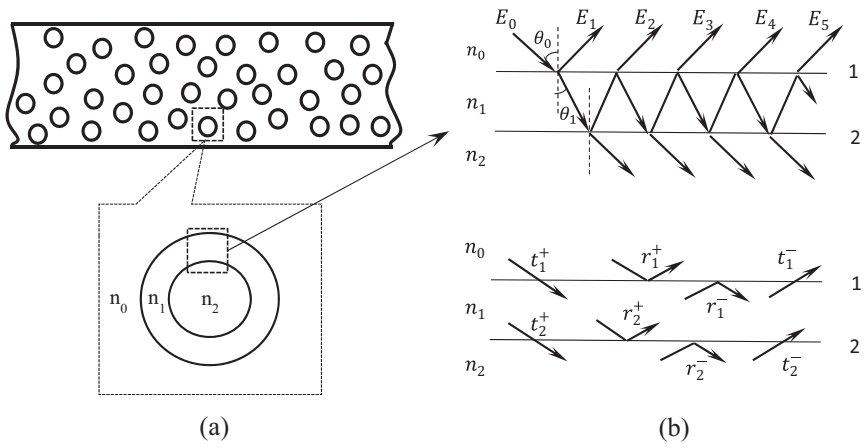

Fig. 1. Schematic diagram of film-coated TiO_2 particles in a paint layer and the light reflection and transmission. (a) TiO_2 particles in paint layer; (b) Light reflection and transmission.

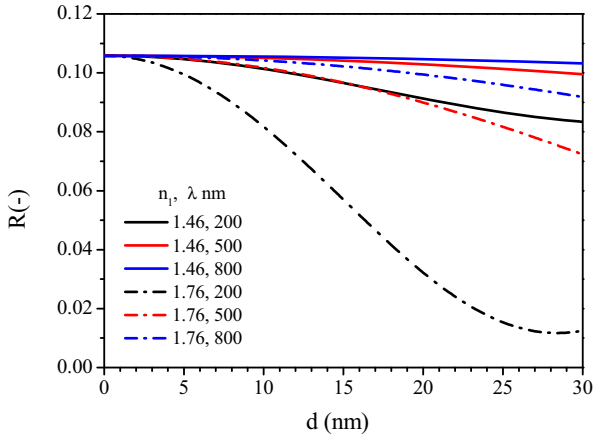

Fig. 2. Light reflectivity as a function of the thickness of silica film (n_1 = 1.46) and alumina film (n_1 = 1.76) for different wavelengths.

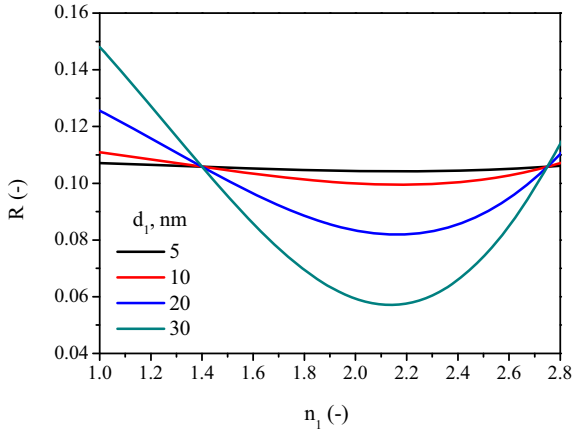

Fig. 3. Light reflectivity as a function of the film refractive index at different film thicknesses.

light (500 nm) and infrared light (800 nm), indicating that the hiding power decreases with the increase of the coating amount on TiO_2 particles and that shorter wavelengths lead to more remarkable hiding power decreases. It is inferred that uncoated TiO_2 particles have the best hiding power. Fig. 3 shows that for different coated film thicknesses, the film reflectivity initially falls and then rises with an increase in the film refractive index. The thicker the film is, the greater the influence is.

By substituting Eqs. (1), (5), (6), and (8) into Eq. (9)

$$\frac{dR}{dn_1} = \frac{dR}{dr_1} \cdot \frac{dr_1}{dn_1} + \frac{dR}{dr_2} \cdot \frac{dr_2}{dn_1} + \frac{dR}{dcos\delta} \cdot \frac{dcos\delta}{dn_1} \quad (9)$$

When $dR/dn_1 = 0$ and $n_1 = 2.15$, the film reflectivity reaches a minimum at a film refractive index of 2.15. For the film refractive index in the range of 1.00–2.15, the film reflectivity decreases as the refractive index increases, while in the range of 2.15–2.80, the film reflectivity increases as the refractive index increases. Supposing the coated film refractive index is 1.40 (organic matrix) or 2.75 (rutile titanium dioxide), the coated TiO_2 particles should have the same reflectivity with uncoated TiO_2 particles, theoretically.

Because the composition and structure determine the apparent refractive index of the films, it is inferred that high light reflectivity, i.e., high hiding power, of coated TiO_2 particles can be achieved by adjusting the composition or the structure of the films coated on the surface of TiO_2 particles. Based on the above analysis, porous SiO_2 and Al_2O_3 coated films can increase the hiding power of coated TiO_2 particles as they have lower apparent refractive indices compared with dense SiO_2- and Al_2O_3-coated films. Because SiO_2 and Al_2O_3 are currently the most widely used coating materials in industrial production, verifying the prediction has a practical and significant purpose. Therefore, experiments were designed and conducted to verify the model's prediction in the following study.

3. Experimental

3.1. Reagents

Commercial TiO_2 particles (technical pure, Jiangsu Hongfeng Titanium Company, China) from the sulfate process, in which TiO_2 particles were produced by the hydrolysis of $TiOSO_4$ and a subsequent calcination, were used in the experiments. The TiO_2 particles have the rutile structure and an average diameter of 300 nm. They were pure without any preliminary treatment. All other chemicals used, namely, $Al_2(SO_4)_3{\cdot}18H_2O$, $Na_2SiO_3{\cdot}9H_2O$, $MgSO_4{\cdot}7H_2O$, $ZnSO_4{\cdot}7H_2O$, $Zr(SO_4)_2{\cdot}4H_2O$, $Ti(SO_4)_2$, NaOH, H_2SO_4, triethanolamine (TEA) and rhodamine-B, were analytical reagent (AR) grade.

3.2. Coating process

Coating experiments were conducted in a flask, and the pH was monitored online using a pH meter. First, 150 g of TiO_2 particles

were dispersed in 300 g of deionized water by an ultrasonic treatment for 30 min to produce a TiO_2 suspension at a concentration of 500 g/L. In the coating and aging processes, the temperature was controlled at 60 °C by a constant temperature bath. The operating procedures were as follows.

(1) SiO_2 single layer coating. 1 mol/L Na_2SiO_3 solution and 1 mol/L H_2SO_4 solution were together titrated into the TiO_2 suspension. The TiO_2 suspension was stirred vigorously, and its pH was controlled at 9 by adjusting the titration rate of the H_2SO_4 solution while keeping the titration rate of the Na_2SiO_3 solution constant. After the titration, the suspension was aged for 2 h under stirring. Then, the coated TiO_2 particles were filtrated and washed three times and dried at 105 °C for 24 h. The amount of SiO_2 coating was 2.0 wt% (SiO_2/TiO_2).
(2) MgO single layer coating. 1 mol/L $MgSO_4$ solution and 4.5 mol/L NaOH solution were together titrated into the TiO_2 suspension. The TiO_2 suspension was stirred vigorously, and its pH was controlled at 5 by adjusting the titration rate of the NaOH solution while keeping the titration rate of the $MgSO_4$ solution constant. After the titration, the suspension was aged for 2 h under stirring. Then, the coated TiO_2 particles were filtrated and washed three times and dried at 105 °C for 24 h. The amount of MgO coating was 2.0 wt% (MgO/TiO_2). The coating amounts and the coating processes of Al_2O_3, ZnO, ZrO_2 and TiO_2 were the same as that of MgO.
(3) Si + Al composite coating. For the Si + Al composite coating, a mixed solution of 0.5 mol/L $Al_2(SO_4)_3$ with a fixed amount of 1 mol/L H_2SO_4 solution was prepared and then together with 1 mol/L Na_2SiO_3 solution was titrated into the TiO_2 suspension at a constant rate. The equivalent coating amounts of SiO_2 and Al_2O_3 were set at 5.0 wt% and 3.0 wt%, respectively. The slurry pH gradually decreased from approximately 9–5 after finishing the titration without control. After filtration, washing and drying as above, the sample was obtained and marked as 5%Si3%Al.

3.3. Evaluation of the weather durability

The weather durability of the film-coated TiO_2 particles was evaluated by examining the degradation of rhodamine-B in the TiO_2 suspension under UV irradiation. Rhodamine-B is a pink, basic dye with molecular formula $C_{28}H_{31}ClN_2O_3$.

Coated TiO_2 particles are still able to degrade rhodamine-B under UV irradiation. The photodegradation kinetics of TiO_2 particles is a typical heterogeneous catalytic reaction which follows the Langmuir adsorption model [22–26]. The rate expression from the Langmuir–Hinshelwood kinetics is often approximated using a first-order kinetic expression when the rhodamine-B concentration is less than 10^{-3} M [27].

$$r = -\frac{dC}{dt} = \frac{k_r KC}{1 + KC} \approx k_r KC = k_{app} C \tag{10}$$

$$\ln\left(C/C_0\right) = -k_{app} t \tag{11}$$

where r is the reaction rate in mg L^{-1} min^{-1}, C is the concentration of rhodamine-B in mg L^{-1}, t is the reaction time in min, k_r is the reaction rate constant in mg L^{-1} min^{-1}, K is the adsorption equilibrium constant in L mg^{-1}, k_{app} is an apparent first-order rate constant in min^{-1}, and C_0 is the initial concentration of the solution after saturation adsorption in mg L^{-1}. At each 30-min interval, the rhodamine-B concentration was measured (C_i, i = 0, 1, . . ., 4). The data points are arranged in a straight fitted line for $\ln(C/C_0)$ versus t, with a slope that is the apparent first-order rate constant. A lower k_{app} indicates a lower degradation rate and lower photocatalytic activity of the TiO_2 particles.

Coated TiO_2 particles (400 mg) were dispersed in 100 mL of rhodamine-B solution with a concentration of 4 mg/L. For a precise measurement, a sufficient adsorption in the suspension was conducted in the dark for 30 min under vigorous stirring and at a constant temperature and air flow rate. Then, the suspension was irradiated under UV light from low pressure mercury lamps (dominant wavelength 254 nm, 32 W) for 120 min [11]. Samples of the suspension were taken every 30 min and centrifuged for 10 min. The suspension supernatant liquid was analyzed with a UV–visible spectrophotometer (TU-1901 Persee, Beijing, China). The characteristic absorbance of rhodamine-B at 554 nm was measured and used to characterize the concentration of rhodamine-B, from which the degradation rate of rhodamine-B was calculated.

3.4. Evaluation of the hiding power

According to the Chinese national testing standards (GB/T 5211.17-1988) [28], the hiding power of the coated TiO_2 particles was measured as follows: 12 g of coated TiO_2 particles were thoroughly ground in an agate mortar, and mixed completely with 100 g of glass beads and 50.5 g of alkyd resin by shaking for 15 min. The ground mixture was coated on the black and white substrates to produce paint layers with different thicknesses by using an automatic coating machine. Then, the paint layers were dried for 24 h at room temperature. The reflectivities of the paint layers on the black and white substrates, which were represented by R_B and R_W, respectively, were measured by a reflectometer at four different positions of the paint layers. Then, the average value R_B/R_W change with the thickness of the wet paint layer was obtained. According to the standard, the R_B/R_W value of the wet paint layer thickness at 100 μm is defined as the hiding power of TiO_2 particles.

3.5. Characterization

Nitrogen adsorption and desorption isotherms at 77 K were obtained using a Quantachrome AUTOSORB-1 automated gas sorption system. In addition, the specific surface area of the coated TiO_2 particles was then calculated according to the BET equation, and the pore volume and pore size distribution of the coated TiO_2 particles were obtained according to the density functional theory (DFT). The morphology and structure of the coated TiO_2 particles were examined with a high-resolution transmission electron microscope (HRTEM, JEM-2011, JEOL Co., Tokyo, Japan).

4. Results and discussion

4.1. Effects of the refractive index of dense film on hiding power

The theoretical calculation indicates that the film refractive index affects the light reflectivity and then affects the hiding power of coated TiO_2 particles. Therefore, the coating of dense films on TiO_2 particles with various oxides (i.e., different refractive indices) was designed and achieved. The SiO_2, Al_2O_3, MgO, ZnO, ZrO_2 and TiO_2 films with refractive indices of 1.46, 1.73, 1.76, 2.00, 2.17, and 2.50, respectively, were coated on TiO_2 particles with a coating amount of 2 wt%, as shown in Fig. 4. From the TEM images, it is seen that the coated films on TiO_2 particles were dense and continuous.

The hiding powers of coated TiO_2 particles with different film refractive indices were measured, as listed in Table 1. Table 1 shows that the film compositions have significant effects on the hiding power (i.e., the light reflectivity). The refractive indices increases from 1.46 to 2.17 (i.e., SiO_2, MgO, Al_2O_3, ZnO and ZrO_2, in turn), and the corresponding hiding powers of coated TiO_2 particles decreases from 93.2 to 91.5, which is in line with the trends of the calculation results. For the film coating with TiO_2 materials, as the TiO_2 film is amorphous, its film refractive index is 2.50. The uncoated TiO_2

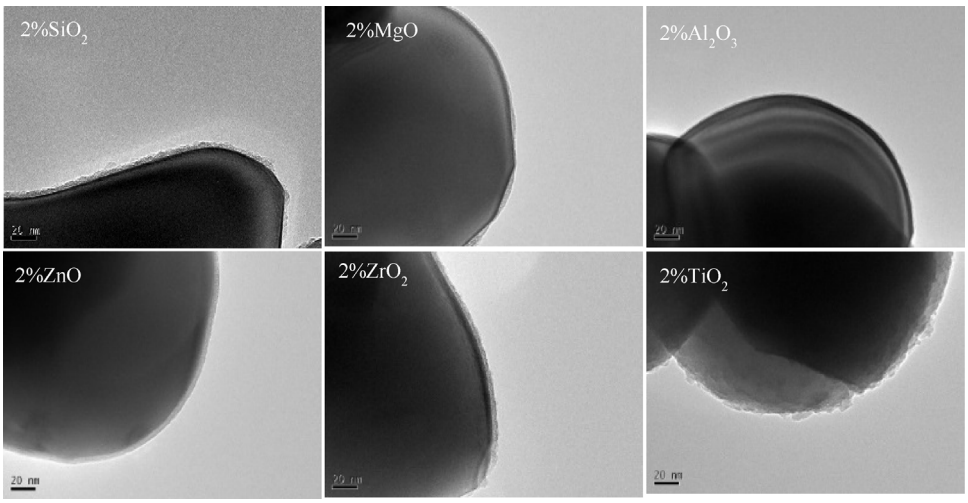

Fig. 4. TEM images of TiO_2 particles coated with different oxide film (2 wt%).

Table 1
Film refractive index and hiding power of TiO_2 particles coated with different oxide films (2 wt%).

Film material	SiO_2	MgO	Al_2O_3	ZnO	ZrO_2	TiO_2	No film
Refractive index (−)	1.46	1.73	1.76	2.00	2.17	2.50	2.75
Hiding power (%)	93.2 ± 0.3	92.8 ± 0.2	92.4 ± 0.3	91.7 ± 0.2	91.5 ± 0.2	92.9 ± 0.3	93.5 ± 0.4

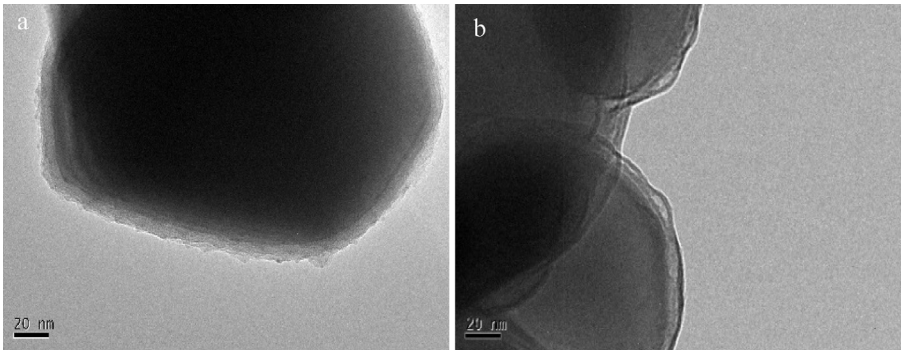

Fig. 5. TEM image of 5%Si3%Al film coated TiO_2 particles. a. no TEA; b. TEA 10 wt%(TEA/film), calcination: 400 °C, 2 h.

particles, regarded as coated TiO_2 particles with a film of rutile titanium dioxide (2 wt%) have a film refractive index of 2.75. The hiding power increases as the film refractive index increases in the range of 2.17–2.75, which also coincides with the trend of the calculation.

4.2. Characteristics of the porous film produced

From the calculations and analysis, it was shown that the TiO_2 particles coated with the porous films have higher hiding powers when the porous films have lower apparent refractive indices. Experiments were designed and conducted to verify the prediction. The porous film coating was conducted by addition of organic templates into the film and subsequent calcination. Because triethanolamine (TEA) can chelate aluminum ions, TEA was added in the process of Si + Al composite coating to produce a porous structure by calcinations. In the absence of TEA, the dense and continuous film of the Si + Al composite was coated on TiO_2 particles, and no porous structure was observed in the film, as shown in Fig. 5(a). Conversely, obvious porous structure was observed in the film with TEA addition and subsequent calcination, as shown in Fig. 5(b).

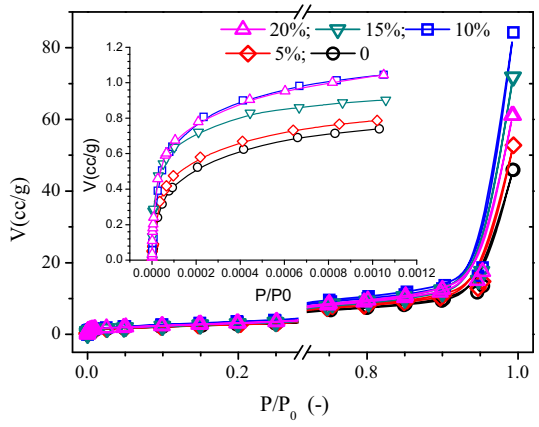

Fig. 6. Nitrogen adsorption and desorption isotherms for 5%Si 3%Al film-coated TiO_2 particles. The inset is the enlarged view of the adsorption isotherms at the low-pressure stage.

Fig. 6 shows the nitrogen adsorption and desorption isotherms for the TiO_2 particles coated with the Si + Al composite. The nitrogen adsorption volume increases slowly as the pressure increases in the

Table 2
Parameters and index of 5%Si 3%Al film-coated TiO_2 particles.

Sample	SSA (m^2/g)	Pore volume (cc/g)	0–6 nm Pore volume (10^{-3}cc/g)	Refractive index	Hiding power (%)	Weather durability, K_{app}·10^3
0	8.72	0.016	3.47	1.486	88.3 ± 0.3	1.7
5%	9.24	0.017	3.72	1.483	89.9 ± 0.2	1.3
10%	11.53	0.021	4.69	1.470	90.8 ± 0.2	1.3
15%	10.00	0.020	3.52	1.485	89.4 ± 0.3	1.6
20%	10.48	0.020	3.93	1.479	90.0 ± 0.3	0.9

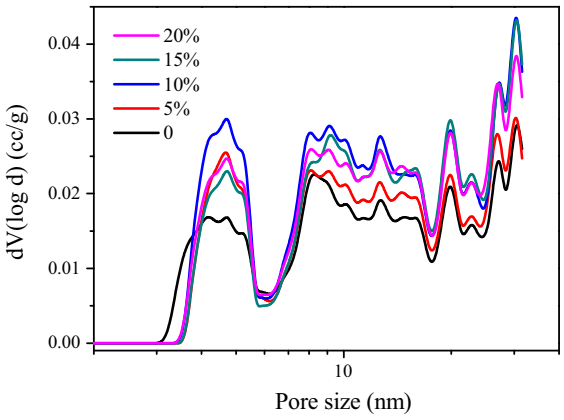

Fig. 7. Pore size distribution of 5%Si 3%Al film-coated on the TiO_2 particles.

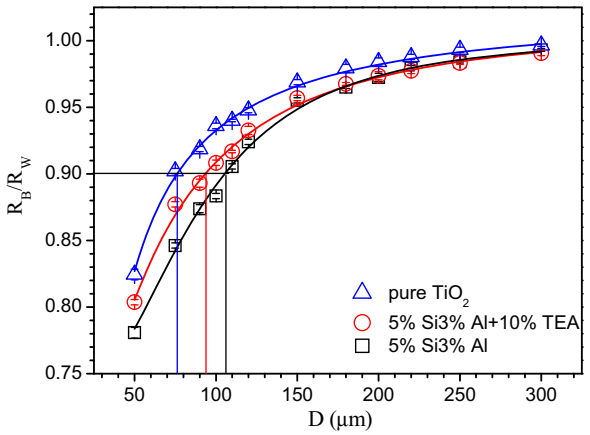

Fig. 8. R_B/R_W as a function of the thickness of the wet paint layer for different TiO_2 particles.

low and middle pressure stages, and the adsorption and desorption curves overlap, which indicates that the pore fraction in the sample is not high. This is because the rutile TiO_2 particles are the main fraction, which have a dense structure that can be considered as the non-porous particles. The inset in Fig. 6 shows an enlarged view of the adsorption isotherms at the low-pressure stage. Different from the film without TEA addition, the film after TEA addition is more porous. Based on the mass estimation, for a coating amount of 8%, the coated film thickness is approximately 8 nm. Thus, the pore size inside the film is generally smaller than 8 nm. The size distribution of the pores was calculated according to the DFT model, as shown in Fig. 7. It is shown that there is a peak of 3–6 nm in the size distribution, which dominates the internal pore size of the film. The film of the coated TiO_2 particles without TEA addition also has a peak of pore size in the 3–6 nm range, much lower than that of the TEA addition.

4.3. Hiding power and weather durability of the TiO_2 particles coated with porous film

To calculate the refractive index of the Si + Al composite coated film, it is assumed that the composite film is composed of silica and alumina. According to the measured pore volume in the 0–6 nm range, the average refractive index is calculated by Eq. (12),

$$n = \frac{n_{SiO_2} \times V_{SiO_2} + n_{Al_2O_3} \times V_{Al_2O_3} + n_{air} \times V_{air}}{V_{SiO_2} + V_{Al_2O_3} + V_{air}} \quad (12)$$

where n_{SiO_2}, $n_{Al_2O_3}$ and n_{air} are refractive indices of silica, alumina and air, respectively; and V_{SiO_2}, $V_{Al_2O_3}$ and V_{air} are the volumes occupied by silica, alumina and air in the film, respectively. The refractive index of the Si + Al composite film changed from 1.486 to 1.470 as TEA was added. Table 2 gives the specific surface area, the pore volume of pores in the 0–6 nm range, the apparent refractive index, the hiding power and the weather durability for the TiO_2 particles coated with the 5%Si3%Al composite film at different TEA amounts. When adding TEA in the coating process, the specific surface area and pore volume of the film-coated TiO_2 particles increased, indicating the pore quantity in the film increased. For TEA addition amounts at 0–10%, the pore volume in the coated film increased as the TEA amounts increased. This resulted in the decreased refractive index of the 5%Si3%Al composite film, leading to the gradual increase of the hiding power of the coated TiO_2 particles from 88.3 to 90.8. This is consistent with the calculation results in Fig. 3 and the experimental results in Table 1.

Table 2 also shows that the apparent degradation rate coefficient of rhodamine-B decreased after adding TEA, indicating that the porous film increased the ability to capture electrons and holes. Therefore, the porous film-coated TiO_2 particles also have a better weather durability.

4.4. The advantages of the porous film coated TiO_2 particles

For uncoated TiO_2 particles (i.e., pure TiO_2), TiO_2 particles coated with the 5%Si3%Al composite and 10% TEA addition (marked as 5%Si3%Al + 10%TEA), and those without TEA addition (marked as 5%Si3%Al), R_B/R_W versus with the thickness of the wet paint layer was obtained, as shown in Fig. 8. The thickness of the wet paint layer has a significant influence on R_B/R_W. When the thickness is less than approximately 150 μm, the ratios R_B/R_W is, in descending order, those of pure TiO_2, 5%Si3%Al + 10%TEA and 5%Si3%Al. When the thickness of wet paint layer increased to 300 μm, the ratios R_B/R_W of all of the TiO_2 particles tends to 1.00.

For a thinner wet paint layer, e.g., thinner than 150 μm, the incident light encounters not so many TiO_2 particles in the transmission path through the paint layer. The reflectivity of the single TiO_2 particle affects R_B/R_W significantly. For a thicker wet paint layer, e.g., thicker than 300 μm, there are a large number of TiO_2 particles in the light path. The reflectivity of a single TiO_2 particle affects R_B/R_W little, leading R_B/R_W for different samples to tend to unity. Fig. 8 shows that setting the ratio $R_B/R_W = 0.90$ requires wet paint layer thicknesses of 75, 93 and 105 μm for pure TiO_2, 5%Si3%Al + 10%TEA and 5%Si3%Al, respectively. Notably, the amount of TiO_2 needed for 5%Si3%Al + 10%TEA (hiding power is 90.8) was reduced by 11.4%, compared with 5%Si3%Al (hiding power is 88.3). Therefore, porous film can increase the hiding power of coated TiO_2 particles, greatly

reducing the dosage of titanium dioxide in the application and the costs.

5. Conclusions

The theoretical calculation and analysis on the light reflection from a plane film model indicates that the apparent refractive index of the coated film affects the film reflectivity significantly, which corresponds to the hiding power of the coated TiO_2 particles. For the refractive index of the coated film in the range of 1.00–2.15, the film reflectivity decreases as the refractive index increases. For the refractive index in the range of 2.15–2.80, the film reflectivity increases as the refractive index increases. These predictions were confirmed experimentally by coating films with various refractive indices on the TiO_2 particles and examining the hiding power of the film-coated TiO_2 particles. The coated films include dense films with different types of oxides, i.e., SiO_2, Al_2O_3, MgO, ZnO, ZrO_2, TiO_2 and the porous films with different pore volume produced by addition of TEA organic templates in the coating process and subsequent calcination. The hiding power of the TiO_2 particles with porous film coatings increased significantly, and the weather durability also increased. The hiding power increase from 88.3 to 90.8 indicated a savings of approximately 10% of the amount of TiO_2 particles needed for reaching the same index of hiding power.

Acknowledgments

The authors wish to express their appreciation for the financial support of this study by the National Natural Science Foundation of China (NSFC No. 21176134) and the National High Technology Research and Development Program (863 Program, No. 2012AA062605).

References

[1] J. Oguma, Y. Kakuma, M. Nishikawa, Y. Nosaka, Effects of silica-coating on the photoinduced hole formation and decomposition activity of titanium dioxide photocatalysts under UV irradiation, Catal. Lett. 142 (2012) 1474–1481.
[2] R. Wang, K. Hashimoto, A. Fujishima, M. Chikuni, E. Kojima, A. Kitamura, M. Shimohigoshi, T. Watanabe, Photogeneration of highly amphiphilic TiO_2 surfaces, Adv. Mater. 10 (1998) 135.
[3] M.L. Taylor, G.E. Morris, R.S. Smart, Influence of aluminum doping on titania pigment structural and dispersion properties, J. Colloid Interface Sci. 262 (2003) 81–88.
[4] L.F. Hakim, D.M. King, Y. Zhou, C.J. Gump, S.M. George, A.W. Weimer, Nanoparticle coating for advanced optical, mechanical and rheological properties, Adv. Funct. Mater. 17 (2007) 3175–3181.
[5] B. Wei, L. Zhao, T. Wang, H. Gao, H. Wu, Y. Jin, Photo-stability of TiO_2 particles coated with several transition metal oxides and its measurement by rhodamine-B degradation, Adv. Powder Technol. 24 (2013) 708–713.
[6] Y. Liu, C. Ge, M. Ren, H. Yin, A. Wang, D. Zhang, C. Liu, J. Chen, H. Feng, H. Yao, T. Jiang, Effects of coating parameters on the morphology of SiO_2-coated TiO_2 and the pigmentary properties, Appl. Surf. Sci. 254 (2008) 2809–2819.
[7] Y. Liu, Y. Zhang, C. Ge, H. Yin, A. Wang, M. Ren, H. Feng, J. Chen, T. Jiang, L. Yu, Evolution mechanism of alumina coating layer on rutile TiO_2 powders and the pigmentary properties, Appl. Surf. Sci. 255 (2009) 7427–7433.
[8] Y. Zhang, H. Yin, A. Wang, M. Ren, Z. Gu, Y. Liu, Y. Shen, L. Yu, T. Jiang, Deposition and characterization of binary Al_2O_3/SiO_2 coating layers on the surfaces of rutile TiO_2 and the pigmentary properties, Appl. Surf. Sci. 257 (2010) 1351–1360.
[9] Y. Zhang, H. Yin, A. Wang, C. Liu, L. Yu, T. Jiang, Y. Hang, Evolution of zirconia coating layer on rutile TiO_2 surface and the pigmentary property, J. Phys. Chem. Solids 71 (2010) 1458–1466.
[10] H. Gao, B. Qiao, T. Wang, D. Wang, Y. Jin, Cerium oxide coating of titanium dioxide pigment to decrease its photocatalytic activity, Ind. Eng. Chem. Res. 53 (2014) 189–197.
[11] L. Zhao, H. Gao, B. Wei, T. Wang, Y. Jin, Evaluation of photocatalytic activity of pigmentary titania, J. Chem. Ind. Eng. (China) 64 (2013) 2453–2461.
[12] S. Fitzwater, J.W. Hook, Dependent scattering-theory—a new approach to predicting scattering in paints, J. Coat. Technol. 57 (1985) 39–47.
[13] J.C. Auger, B. Stout, Dependent light scattering in white paint films: clarification and application of the theoretical concepts, J. Coat. Technol. Res. 9 (2012) 287–295.
[14] N. Veronovski, M. Lesnik, D. Verhovsek, Surface treatment optimization of pigmentary TiO_2 from an industrial aspect, J. Coat. Technol. Res. 11 (2014) 255–264.
[15] Z. Tang, Production and Environmental Management of Titanium Dioxide, Chemical Industry Press, Beijing, 2000.
[16] P. Alphonse, B. Faure, Synthesis of highly porous alumina-based materials, Microporous Mesoporous Mater. 181 (2013) 23–28.
[17] H.Y. Zhu, J.D. Riches, J.C. Barry, Gamma-alumina nanofibers prepared from aluminum hydrate with poly(ethylene oxide) surfactant, Chem. Mater. 14 (2002) 2086–2093.
[18] M. Takbiri, K.J. Jozani, A.M. Rashidi, H.R. Bozorgzadeh, Preparation of nanostructured activated alumina and hybrid alumina-silica by chemical precipitation for natural gas dehydration, Microporous Mesoporous Mater. 182 (2013) 117–121.
[19] V.R.R. Goparaju, M.L. Ashley, Titanium dioxide pigments and manufacturing method, US, US8840719, 2014.
[20] Y. Tang, G. Hu, An analysis of the reflectivity and anti-reflective film, J. Huaiyin Inst. Technol. (China) 17 (2008) 86–88.
[21] M. Born, E. Wolf, Principles of Optics: Electromagnetic Theory of Propagation, Interference and Diffraction of Light, seventh ed., CUP, Cambridge, 1999.
[22] A. Fujishima, X. Zhang, D.A. Tryk, TiO_2 photocatalysis and related surface phenomena, Surf. Sci. Rep. 63 (2008) 515–582.
[23] D.S. Bhatkhande, V.G. Pangarkar, A. Beenackers, Photocatalytic degradation for environmental applications—a review, J. Chem. Technol. Biotechnol. 77 (2002) 102–116.
[24] A.L. Linsebigler, G.Q. Lu, J.T. Yates, Photocatalysis on TiO_2 surfaces—principles, mechanisms, and selected results, Chem. Rev. 95 (1995) 735–758.
[25] M.A. Fox, M.T. Dulay, Heterogeneous photocatalysis, Chem. Rev. 93 (1993) 341–357.
[26] J.M. Herrmann, Heterogeneous photocatalysis: fundamentals and applications to the removal of various types of aqueous pollutants, Catal. Today 53 (1999) 115–129.
[27] Y. Li, S. Sun, M. Ma, Y. Ouyang, W. Yan, Kinetic study and model of the photocatalytic degradation of rhodamine B (RhB) by a TiO_2-coated activated carbon catalyst: effects of initial RhB content, light intensity and TiO_2 content in the catalyst, Chem. Eng. J. 142 (2008) 147–155.
[28] Comparison of contrast ratio (hiding power) of white pigments (GB/T 5211.17) (1988).